

Multicolor Luminescence of a Polyurethane Derivative Driven by Heat/Light-Induced Aggregation

Nan Jiang, Ke-Xin Li, Wei Xie, Shu-Ran Zhang, Xin Li, Yue Hu, Yan-Hong Xu,* Xing-Man Liu,* and Martin R. Bryce*



Cite This: *Macromolecules* 2023, 56, 7721–7728



Read Online

ACCESS |

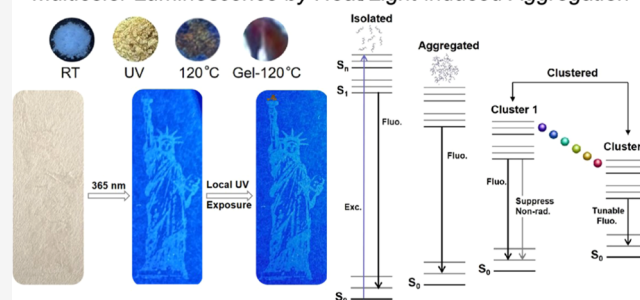
Metrics & More

Article Recommendations

Supporting Information

ABSTRACT: The study of aggregate formation and its controllable effect on luminescence behavior has a far-reaching influence in establishing a universal aggregation photophysical mechanism. In this paper, we obtained clusters with different extents of aggregation by heat-induced or light-triggered aggregation of a new polyurethane derivative (PUE). The controllable regulation of multicolor fluorescence of a single (nondoped) polymeric material is realized. The luminescence behavior of PUE varies with microscopic control of the aggregation structure. Compared with the powder state, the enhanced atom–atom and group–group interactions of PUE-gel effectively limit the nonradiative transitions in the excited state and result in a red-shift in emission. This work avoids complex organic synthesis and demonstrates a simple strategy to induce aggregation and regulate the emitting color of macromolecules, providing a template for developing new materials for multicolor fluorescence. In addition, a pattern was constructed with encryption, anticounterfeiting, and information transmission functions which provide a proof-of-concept demonstration of the practical potential of PUE as a smart material.

Multicolor Luminescence by Heat/Light-induced Aggregation



1. INTRODUCTION

Ever since the 1660s when Newton advanced the understanding of the color of light and ushered in a new era of scientific endeavor, humans have continually pursued new light-induced phenomena and applications. Compared with small organic molecules that often require complex chemical synthesis and tedious purification, macromolecular luminescent materials have a wide range of applications in the fields of display technologies, photochemical sensing, information storage, and photoelectric devices because of their advantages such as easy functionalization, low-cost high-volume production, and diverse molecular conformations.^{1–5} The luminescence of molecules is not only related to their intrinsic molecular structure but also to their aggregation state.^{6–10} Thus, the in-depth study of aggregate luminescence is of great significance to guide further developments in functional macromolecular materials. Polyurethanes are a class of block polymers formed by alternating soft and rigid segments incorporating urethane (carbamate) links.^{11–13} Such a structure not only provides a large number of lone pair electrons but is also rich in hydrogen bonding and other noncovalent interaction sites.^{14–18} Polyurethane is a suitable material template for in-depth studies of complex spatial interactions and aggregation's luminescence behavior.

In this work, we designed and synthesized a polyurethane derivative. By exploiting heat/light-induced aggregation, micro-

scopic control of the structure and remote control of the macroscopic luminescence behavior of the material have been realized. Thermochromic/photochromic functional materials exhibit dynamic multicolor fluorescence changes under heat/light stimulation.^{19–23} Compared with other stimulus-response materials, they have the advantage of contact-less control,^{24–26} which endows them with great potential applications in the fields of optical response materials,^{27–29} hologram photography,^{30–32} encryption, and anticounterfeiting.^{33–35} There have been some studies on thermo-photoluminescent oligo/polyurethanes, but most of them are composites, such as doping with metal ions, SiO₂, or rare-earth luminous complexes.^{36–40} There are also several pure polyurethanes with thermal/photochromic properties obtained by covalent linking or simply doping with monomers that can undergo isomerization.^{41–45} However, such systems are often plagued by aggregation-caused quenching (ACQ) effects. For example, after gelation, the dense three-dimensional network would impose significant steric hindrance, which makes it challenging

Received: July 8, 2023

Revised: September 4, 2023

Published: September 29, 2023



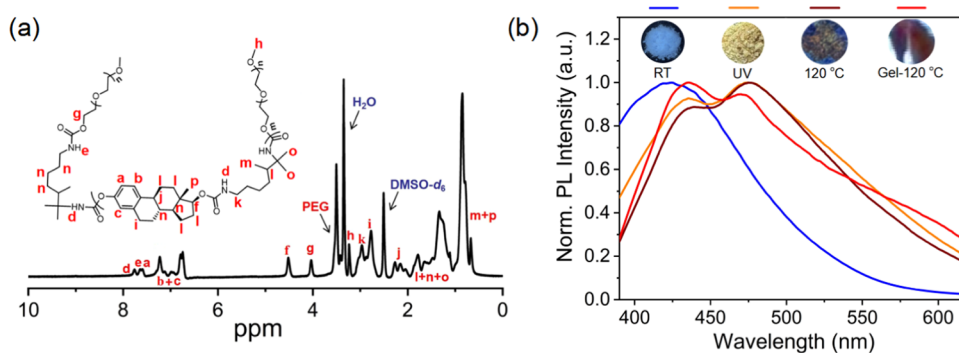


Figure 1. (a) Molecular structure and ^1H NMR spectrum of **PUE** in $\text{DMSO-}d_6$, with residual proton resonance in $\text{DMSO-}d_6$ ($\delta = 2.5$ ppm). (b) PL spectra of **PUE-powder** at room temperature; after ultraviolet radiation; and heated at 120°C and **PUE-gel** heated at 120°C ($\lambda_{\text{ex}} = 365$ nm). Inset: images of these samples under a 365 nm UV lamp.

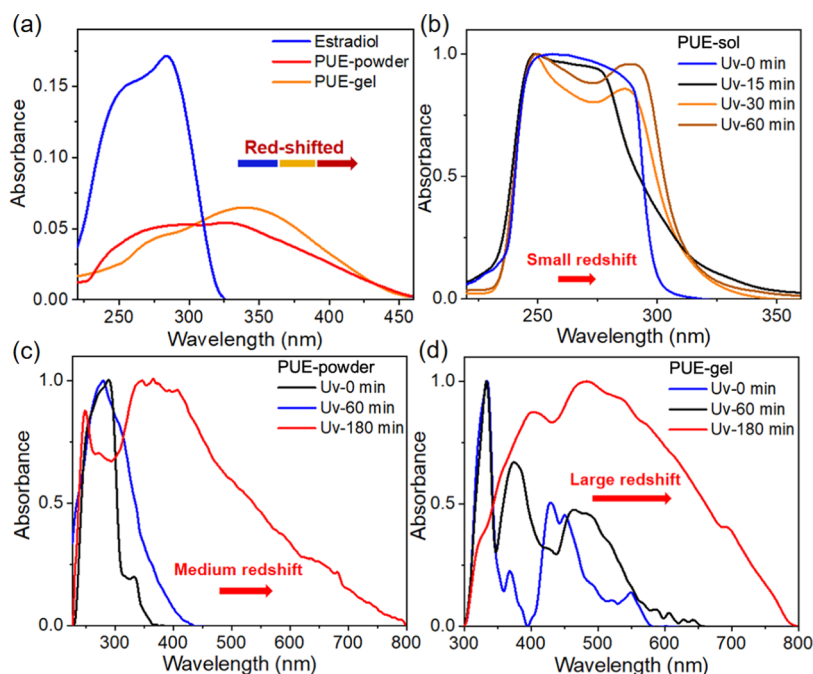


Figure 2. (a) UV–vis spectra of estradiol monomer, **PUE-powder**, and **PUE-gel**. (b) UV–vis spectra of **PUE-sol** before and after ultraviolet radiation. (c) UV–vis spectra of **PUE-powder** before and after ultraviolet radiation. (d) UV–vis spectra of **PUE-gel** before and after ultraviolet radiation.

to isomerize the chromophores.⁴⁶ As a result, they cannot exhibit thermal or photochromic behavior in the aggregate state, which greatly limits the application of such materials.

Herein, we report a new nonconjugated polyurethane derivative (**PUE**) based on estradiol. Estradiol was chosen as a readily available backbone unit to provide some defined aliphatic structural rigidity in the polymer. **PUE** shows thermal and photochromic responses through simple aggregation changes. Combining the advantages of gelation- and aggregation-induced emission (AIE), **PUE**'s multicolor fluorescence range broadens from blue to red. As an AIE system without typical π -conjugated units, a systematic study of luminescence properties of **PUE** in solution, powder, and gel was undertaken to probe the relationship between noncovalent interactions in different aggregation states and the macroscopic luminescence properties of the material. The development of AIE soft materials of this type with multicolor luminescence will facilitate the construction of new advanced multifunctional optical materials.

2. RESULTS AND DISCUSSION

2.1. Synthesis. The synthesis and characterization of **PUE** are described in Section 4 and in the Supporting Information (SI). Figure 1a shows the molecular structure and ^1H NMR spectrum of **PUE**.

2.2. Physical Properties. As shown in Figure S2 in the SI, based on the emission spectra, the estradiol monomer could not be excited as a chromophore to emit visible light. However, after polymerization, the nonconjugated product (**PUE**) based on estradiol displayed typical cluster aggregation-induced emission characteristics. As shown in Figure S3a in the SI, as the excitation wavelength increased from 320 to 540 nm, the fluorescence emission of the **PUE-powder** gradually redshifted. Figure S3b shows that the emission intensity of **PUE-sol** in the trichloromethane solution increased with increasing concentration within the range of 1.56×10^{-5} to 5×10^{-4} M. These results indicate that **PUE** is a cluster luminescent material with excitation dependence and concentration dependence, features typical of AIE materials.⁴⁷ Figure 2a

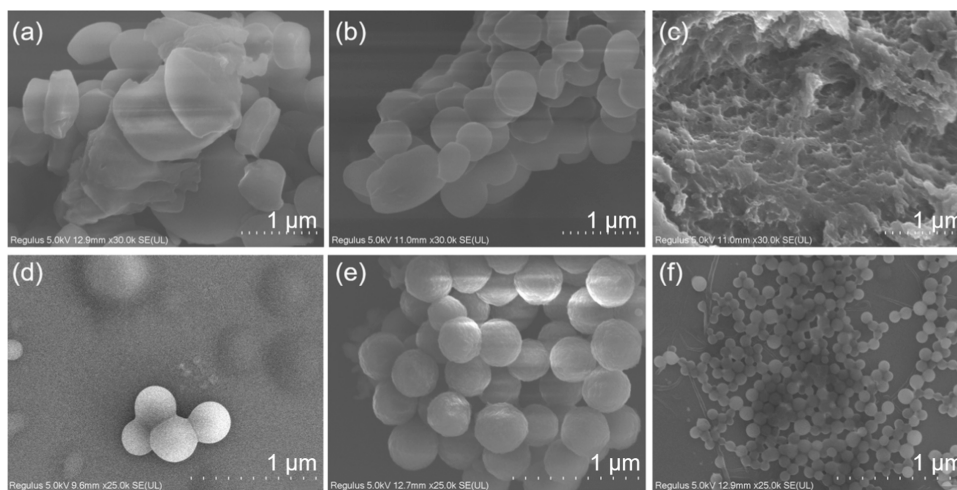


Figure 3. SEM images of PUE-powder dispersed in ethanol (a) at room temperature (b) heated at 85 °C and (c) heated at 120 °C. SEM images of PUE-gel dispersed in ethanol (d) at room temperature (e) heated at 85 °C and (f) heated at 120 °C.

shows that the estradiol monomer does not show absorption in the visible region. However, after the polymerization reaction, the absorption of the material was greatly shifted into the visible region. After gelation, due to the unique cross-linked network structure, the absorption maximum of the PUE-gel was further red-shifted.

Surprisingly, PUE exhibits multicolor fluorescence driven by heat or ultraviolet (UV) light over a large color gamut span (Figure 1b), which is consistent with the absorption spectra (Figures 2 and S4). Figure 2b–d shows that the absorption of PUE-sol, PUE-powder, and PUE-gel varies greatly after UV irradiation, indicating that PUE has obvious photochromic properties. Compared with PUE-sol, the absorption range of PUE-powder and PUE-gel was much larger, implying that aggregation can amplify the photochromic effect. For solution, powder, and gel samples, different heating/illumination temperatures and times are required to achieve aggregation. Weakly aggregated solution samples of PUE-sol need only 1 h of illumination to change the fluorescence from blue to yellow (Figure S9a). For the powder, the fluorescence change can be observed by heating for 3 h, but for the gel sample with strong initial aggregation, a longer time (5 h) is required to achieve the fluorescence transition. It is worth noting that heating samples at 80 °C for a few hours and then placing them into a 120 °C oven will achieve a fluorescence transition faster than simply heating at 120 °C, implying that the aggregation behavior is gradual and requires time for the physical change to occur.

2.3. Mechanism of Multicolor Luminescence. In order to explore the mechanism of the thermochromism, the ^1H NMR spectra (Figure S5a) showed that the chemical structure of PUE did not change after high-temperature treatment and ultraviolet irradiation, which ruled out the possibility that the fluorescence changes are due to isomerization or degradation of the molecular structure. However, heating has an impact on the aggregation behavior at the supramolecular level of physical change (Figures S6 and 3). We propose, therefore, that the unusual thermal/photochromic properties of PUE arise from changes in the molecular aggregation state of PUE: the discrete molecular chains of PUE do not emit at long wavelength, but the aggregates of PUE in the solid powder and gel state can achieve a higher degree of spatial electron conjugation and finally obtain the long-wavelength emission, which is a feature

of nonconjugated cluster aggregation luminous materials. To probe this mechanism, the material morphology was studied by scanning electron microscopy (SEM). PUE-powder at room temperature and after heating was dispersed in ethanol. SEM results (Figure 3a–c) showed that compared to room temperature, the sample heated at 85 °C showed a denser nanosphere microstructure at the same magnification. In addition, PUE-powder treated at 120 °C showed a more concentrated gelated cross-linked structure. This is consistent with the thermochromic behavior of PUE-powder: the more it aggregates, the more red-shifted the emission. Figure S6c,d shows that UV irradiation can also induce nanoaggregation. The excitation energy generated by UV light can induce the formation of aggregates,⁴⁶ and in addition, significant photo-thermal interactions can be produced by UV light irradiation, which can also promote nanoaggregation.⁴⁸

Due to the appearance of nanoaggregates, the energy level of PUE is split, gradually reducing the gap, and, concomitantly, the luminescence is gradually red-shifted. We suggest that the dispersion medium in the gel network provides room for the clusters to move and helps regulate their luminous properties by manipulating the intramolecular motion. Therefore, PUE-gel has more obvious thermochromic and photochromic properties than PUE-powder. Figure 3d–f shows the SEM studies of the aggregation behavior of the gel. At room temperature, PUE-gel presents a dispersed nanosphere structure. However, after heating at 85 °C, a very tightly clustered “bunch of grapes”-like nanosphere structure is observed (Figure 3e), and the uneven surface of the nanospheres could be clearly observed at higher magnification (Figure S6a). After heating to 120 °C, the nanospheres split into smaller nanospheres and even formed single-ended aggregated nanorods (Figure S6b). The above experimental results prove that thermogenic and photochromic processes occur through nanoaggregation of PUE. A large number of electronic interactions between chromophores enhance the overlap of excited-state orbitals, leading to energy-level splitting. Clusters with different extents of aggregation bring different energy gaps, ultimately leading to the multicolor emission behavior of PUE.

We propose that the aggregation behavior of PUE is due to its conformational changes. There are many noncovalent interaction sites on the PUE chain, which are critical for

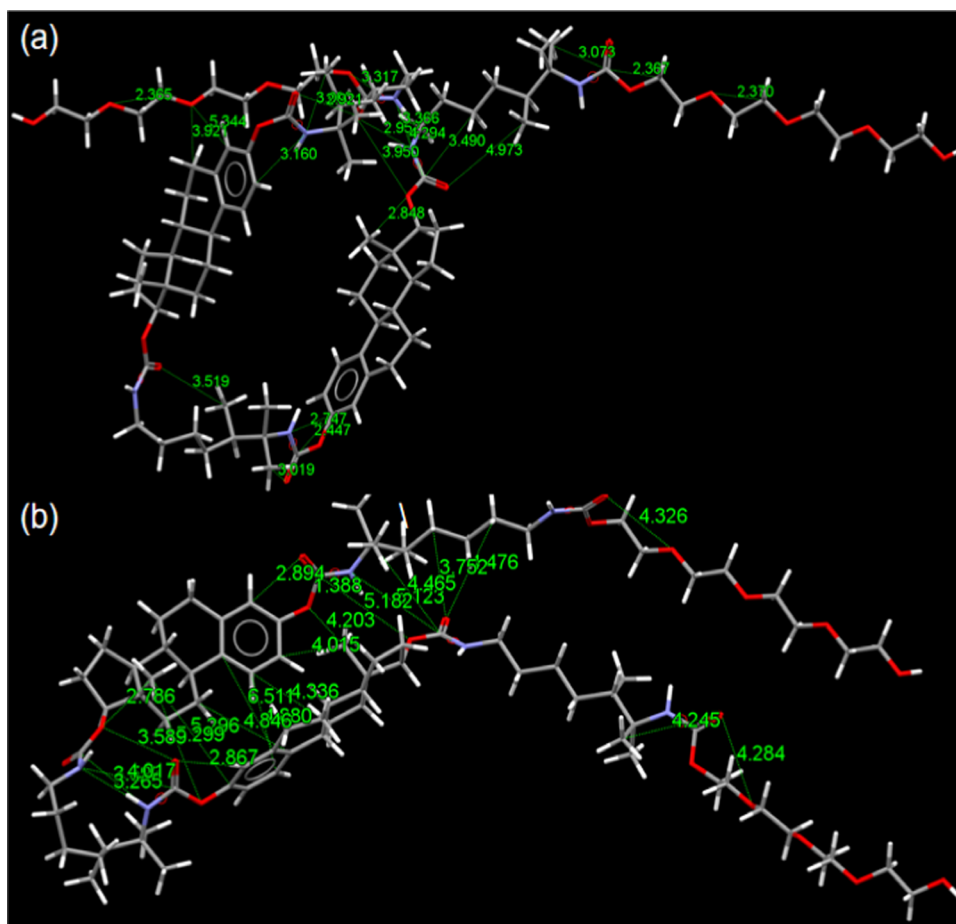


Figure 4. Theoretical calculations based on the single PUE chain by the B3LYP/6-31g(d) method in different degree folding modes. (a) Helical conformation. (b) Folded conformation.

aggregation-induced polychromatic fluorescence. The crystallization rate of PUE-powder before and after heating was studied by wide-angle X-ray diffraction (WAXD). As shown in Figure S5b, the broad peak at 2θ around 16.8° corresponds to the PU skeleton, as reported previously, indicating that both crystalline and amorphous structures exist in PUE samples.¹⁸ The diffraction peak intensity of PUE-powder increased and widened with increasing temperature, indicating that the chains' conjugation length increased with a transition to a more conformational order. At room temperature, due to the flexible chain structure and extensive intramolecular hydrogen bonding, the chains are relatively twisted and coiled. However, upon heating, a substantial number of intrachain heat-sensitive hydrogen bonds break, and the PUE chains partly extend. This favors the increase of interchain interactions, which dominate the strong aggregation behavior. Thus, a large number of disordered amorphous chains are transformed into more ordered crystalline conformations with increasing conjugation length, red-shifting the emission, in agreement with the PL results discussed above (Figure 1b).

Analysis of the Fourier transform infrared (FT-IR) spectra provides strong support for this conjecture. As shown in Figure S7, the FT-IR spectra of PUE-powder at 0 and 120°C showed that the N–H stretching peaks were significantly broader and shifted from ν_{max} 3341 to 3429 cm^{-1} after heating. At the same time, the C=O bond moved from ν_{max} of 1718 to 1628 cm^{-1} . PUE-powder, PUE-gel, and PUE-sol after UV irradiation showed changes similar to those of PUE-powder after heating

(Figure S8). These wavenumber changes show that the hydrogen bond between the N–H and C=O units weakened after exposure to heat and UV light. This can be explained by a loose aggregated structure with predominant intramolecular H-bonds at room temperature. After heating or UV irradiation, these bonds are weakened or destroyed, and noncovalent interactions between adjacent chains become dominant, thereby enhancing the aggregation of PUE chains through noncovalent spatial conjugation, which causes the luminescence to red-shift further. A detailed discussion is in Section 4.4.

Furthermore, the FT-IR and emission spectra of the photochromic PUE solution have been studied after storage in daylight at room temperature for 1 day (Figures S8d and S9a). It was found that PUE-sol returned to the blue fluorescence state it had before exposure to UV light and the intramolecular hydrogen bonding had also been restored. PUE-sol has a faster color-changing/color-reverting process than PUE-gel (Figures S8c and S9b); the latter has increased stability after photochromism because of the tight three-dimensional cross-linked network structure of the gel (Figure S8).

In order to better understand the cluster aggregation luminescence properties of PUE, the luminescence lifetime and quantum efficiency (QY) of PUE-sol, PUE-powder, and PUE-gel were recorded (Table S1). From the analysis of the experimental results, it can be seen that UV light can greatly increase the fluorescence lifetime of PUE-sol, which may be

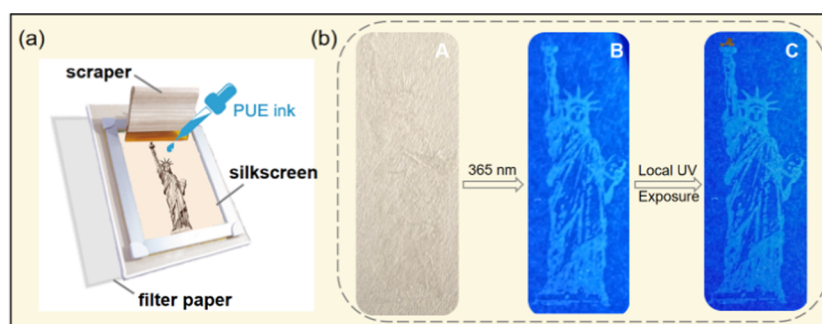


Figure 5. Schematic illustration of the application process for screen printing. (a) Schematic diagram of a screen-printing device. (b) Silkscreen image of the Statue of Liberty: (A) under daylight; (B) under 365 nm UV lamp; and (C) after local UV exposure for 10 min.

due to the formation of various clusters, resulting in energy-level splitting and the increase of radiative transition channels. For powdered samples, the QY and lifetimes are significantly reduced after heating, which may be because of the formation of multitype clusters in the solid aggregation state; although the energy level is split, this also enhances the radiative transition between the n_{th} singlet electron excitation states (S_n) to the ground (S_0) state and weakens the rigidity of the material, finally leading to the decrease of lifetime and QY. For the gel sample, the existence of solvent molecules in the initial state obstructs the electronic communication between the luminous clusters, so the lifetime and efficiency are low. However, after heating at 80 °C and the evaporation of solvent molecules, the efficiency of PUE-gel reaches 8%, which is because compared with the powder sample, the efficiency of PUE-gel reaches 8%. This is because the initial PUE-gel molecule has a tighter structure, and when the solvent evaporates, the space electrons are fully conjugated, resulting in a significant increase in efficiency. However, further heating will cause the sample to undergo a similar process to the powder sample, so the efficiency becomes lower again. We speculate that there may be different rules for the aggregation behavior of cluster luminescent materials for different initial states of samples, which may lead to unexpected results, such as a large increase in luminous efficiency. Further exploration of this aspect is beyond the scope of the present manuscript, but it can be expected that more detailed explanations will be established in the future. These results provide an effective bridge for further understanding the relationship between molecular aggregation and macro-luminescence properties.

2.4. Theoretical Calculations. In order to gain insight into the origin of the aggregation-induced polychromatic fluorescence of PUE, the photophysical mechanisms involved were further explored at the molecular level. Density functional theory (DFT) was used to optimize the PUE chains under different folding modes. The corresponding through-space interaction (TSI) diagrams are visualized in Figures 4 and S10–S12. Due to the softness of the polymer chains, there were strong intramolecular TSIs in a single PUE chain (e.g., C–H $\cdots\pi$; C–H \cdots O=C; $\pi\cdots\pi$; C–H \cdots N; N–H \cdots N). Clearly, aggregation behavior mainly depends on intermolecular rather than intramolecular interactions.⁴ Thus, these strong intrachain TSIs result in loose aggregation structures, and the original PUE shows blue fluorescence. However, after heating or UV irradiation, intrachain interactions such as hydrogen bonds were destroyed (Figure S8), PUE chains partially extended, and the conjugation also extended to a certain extent. More importantly, a large number of noncovalent interactions and

short contacts occur between adjacent PUE chains, especially in the alkoxy end regions (Figure S12). These interchain TSIs and short contacts are conducive to the formation and stability of large clusters.

2.5. Application. Thanks to the excellent solution processability, PUE can be used as a screen-printing ink. Based on the thermal/photochromic properties, PUE can be applied for encryption. An image of the Statue of Liberty printed on a filter paper through a screen-printing mold using PUE-gel as the ink is shown in Figure 5a. Figure 5b shows that under daylight, the pattern is barely visible on the filter paper. However, the fluorescent blue pattern of the Statue can be observed under a 365 nm UV lamp. When localized ultraviolet radiation is applied for 10 min, the torch in Lady Liberty's hand lights up (Figure 5b(C))! This proof-of-concept model has the advantages of antireplication and high security, providing a new design for intelligent anticounterfeiting and information storage materials.

3. CONCLUSIONS

In summary, we have reported a novel multicolor aggregation-induced luminescence polyurethane derivative PUE driven by heat/light, successfully achieving noncontact multicolor fluorescence regulation of a monomolecular material. The luminescence behavior and the thermochromic/photochromic characteristics were systematically studied by photophysical experiments, FT-IR spectroscopy, WAXD experiments, and theoretical calculations. The flexible structure of PUE chains allows the regulation of multiple noncovalent intramolecular/intermolecular interactions of PUE. Under the stimulation of heat or UV light, hydrogen bonds in PUE chains break, curved molecular chains become extended, and conjugation can be increased. In addition, driven by a large number of noncovalent interactions, PUE chains further aggregate to form luminous clusters with varying degrees of aggregation. A large number of electronic interactions lead to exciton orbital overlap and energy-level splitting. Clusters with different degrees of aggregation bring different gaps and finally contribute to the multicolor emission behavior of PUE. The multicolor emission of the gel with heat- and light-induced aggregation is versatile for further developments in multifunctional stimulus-responsive macromolecules. Due to the excellent adhesive and high photochromic stability, PUE-gel can form fluorescent staining traces that are retained for a period of time. Therefore, PUE-gel has a broad application prospect in luminescent paints for security applications, signage, commodity items, automobiles, ships, or aircraft.

4. EXPERIMENTAL SECTION

4.1. Synthesis. PUE was prepared according to the following procedure. A mixture of estradiol (0.7136 g, 2.62 mmol), poly-(ethylene glycol) monomethyl ether ($M_w = 200 \text{ g mol}^{-1}$; 0.396 g, 1.98 mmol), anhydrous THF (8 mL), trimethylhexa-1,6-diyl diisocyanate (0.7590 g, 3.61 mmol), and 1,4-diazabicyclooctane triethylenediamine (DABCO) (0.012 g, 0.06 mmol) was stirred in N_2 atmosphere at 68 °C for 8 h until the clear solution became viscous, indicating that oligo/polymerization had occurred. After cooling to room temperature, the mixture was added to excess *tert*-butyl methyl ether drop by drop for reverse precipitation to give a product, which was then dried under a vacuum at room temperature for 24 h to obtain polyurethane PUE (1.21 g, 65% yield). $^1\text{H NMR}$ (400 MHz, $\text{DMSO}-d_6$, δ [ppm]): 7.76 (s, 2H), 7.64 (s, 2H), 7.59 (s, 1H), 6.65–7.35 (broad, 2H), 4.03 (s, 4H), 3.39–3.59 (broad, PEG protons), 3.23 (s, 6H; PEG terminal $-\text{OCH}_3$ protons), 1.96–2.36 (broad, 2H), 1.05–2.35 (broad, 30H), 0.6–1.05 (broad, 9H). FT-IR: 3341 cm^{-1} (N–H), 2871 cm^{-1} and 2939 cm^{-1} ($-\text{CH}_2-$ asymmetric and symmetric stretch), 1718 ($\text{C}=\text{O}$), 1140 cm^{-1} ($\text{C}-\text{O}-\text{C}$ stretch PEG). $M_n = 3696 \text{ g mol}^{-1}$, $M_w = 4866 \text{ g mol}^{-1}$, PDI = 1.32.

4.2. Photophysical Characterization. The UV–vis absorption spectra were recorded on a Shimadzu UV-3100 spectrophotometer. The fluorescence spectra were recorded on a Hitachi model F-4700 spectrometer. The fluorescence lifetimes (τ) and fluorescence quantum yields (Φ_f) were recorded using an Edinburgh Instruments FLS-1000 spectrometer. The luminescence photos were taken by an iPhone 14 pro under the irradiation of a hand-held UV lamp at room temperature.

4.3. Experimental Sample Preparation. PUE-sol was prepared by dissolving PUE-powder (30 mg) in dimethyl sulfoxide (DMSO) solution (2 mL). PUE-gel was prepared by dissolving 5 wt % PUE-powder in DMSO under heating, and after cooling to room temperature, PUE-gel was obtained.

4.4. Theoretical Calculations. The density functional theory (DFT) calculations were performed by using the Gaussian program. Two repeating molecular units with H as the chain ends were selected as the computational model. The structures of polyurethane with different conformations (helical and folded) were optimized at the B3LYP/6-31G* level with Gaussian 09 (D.01). The short contacts and hydrogen-bonding interactions were obtained at the B3LYP/6-311G** level with Gaussian 16 Revision B01.

■ ASSOCIATED CONTENT

SI Supporting Information

The Supporting Information is available free of charge at <https://pubs.acs.org/doi/10.1021/acs.macromol.3c01345>.

Additional structural characterization; copies of NMR spectra; FT-IR spectra; additional photophysical data; scanning electron microscopy (SEM); and wide-angle X-ray diffraction (WAXD) data (PDF)

■ AUTHOR INFORMATION

Corresponding Authors

Yan-Hong Xu – Key Laboratory of Preparation and Applications of Environmental Friendly Materials, Key Laboratory of Functional Materials Physics and Chemistry of the Ministry of Education, Jilin Normal University, Changchun 130103, China; orcid.org/0000-0002-9930-587X; Email: xuyh198@163.com

Xing-Man Liu – School of Chemistry and Chemical Engineering, Ningxia University, Yinchuan 750021, China; Email: liuxm2020@nxu.edu.cn

Martin R. Bryce – Department of Chemistry, Durham University, Durham DH1 3LE, U.K.; orcid.org/0000-0003-2097-7823; Email: m.r.bryce@durham.ac.uk

Authors

Nan Jiang – Key Laboratory of Preparation and Applications of Environmental Friendly Materials, Key Laboratory of Functional Materials Physics and Chemistry of the Ministry of Education, Jilin Normal University, Changchun 130103, China

Ke-Xin Li – Key Laboratory of Preparation and Applications of Environmental Friendly Materials, Key Laboratory of Functional Materials Physics and Chemistry of the Ministry of Education, Jilin Normal University, Changchun 130103, China

Wei Xie – Key Laboratory of Preparation and Applications of Environmental Friendly Materials, Key Laboratory of Functional Materials Physics and Chemistry of the Ministry of Education, Jilin Normal University, Changchun 130103, China

Shu-Ran Zhang – Key Laboratory of Preparation and Applications of Environmental Friendly Materials, Key Laboratory of Functional Materials Physics and Chemistry of the Ministry of Education, Jilin Normal University, Changchun 130103, China

Xin Li – Key Laboratory of Preparation and Applications of Environmental Friendly Materials, Key Laboratory of Functional Materials Physics and Chemistry of the Ministry of Education, Jilin Normal University, Changchun 130103, China

Yue Hu – Key Laboratory of Preparation and Applications of Environmental Friendly Materials, Key Laboratory of Functional Materials Physics and Chemistry of the Ministry of Education, Jilin Normal University, Changchun 130103, China

Complete contact information is available at:

<https://pubs.acs.org/10.1021/acs.macromol.3c01345>

Notes

The authors declare no competing financial interest.

■ ACKNOWLEDGMENTS

The work was funded by the Science and Technology Development Program of Jilin Province (YDZJ202301-ZYTS305, YDZJ202201ZYTS354, and YDZJ202201-ZYTS355), the Research Program on Science and Technology from the Education Department of Jilin Province (Grant Nos. JJKH20220433KJ and JJKH20220441KJ), the Key Research and Development Program of Ningxia (Special program for Talent introduction, 2022BSB03074), and NSFC (Grant No. 21975103). M.R.B. thanks EPSRC grant EP/L02621X/1 for funding.

■ REFERENCES

- (1) Abdollahi, A.; Dashti, A. Photosensing of Chain Polarity and Visualization of Latent Fingerprints by Amine-Functionalized Polymer Nanoparticles Containing Oxazolidine. *Eur. Polym. J.* **2023**, *191*, No. 112038.
- (2) Zhang, X. J.; Gao, R. T.; Kang, S. M.; Wang, X. J.; Jiang, R. J.; Li, G. W.; Zhou, L.; Liu, N.; Wu, Z. Q. Hydrogen-Bonding Dependent Nontraditional Fluorescence Polyphenylallenes: Controlled Synthesis and Aggregation-Induced Emission Behaviors. *Polymer* **2022**, *245*, No. 124712.
- (3) Wang, T.; Su, X.; Zhang, X.; Huang, W.; Huang, L.; Zhang, X.; Sun, X.; Luo, Y.; Zhang, G. A Combinatory Approach towards the Design of Organic Polymer Luminescent Materials. *J. Mater. Chem. C* **2019**, *7*, 9917–9925.

- (4) Hu, R.; Xin, D. H.; Qin, A. J.; Tang, B. Z. Polymers with Aggregation-Induced Emission Characteristics. *Acta Polym. Sin.* **2018**, *2*, 132–144.
- (5) Xu, L.; Hu, R.; Tang, B. Z. Room Temperature Multicomponent Polymerizations of Alkynes, Sulfonyl Azides, and Iminophosphorane toward Heteroatom-Rich Multifunctional Poly(Phosphorus Amidine)s. *Macromolecules* **2017**, *50*, 6043–6053.
- (6) Würthner, F. Aggregation Induced Emission (AIE): A Historical Perspective. *Angew. Chem., Int. Ed.* **2020**, *59*, 14192–14196.
- (7) Chu, B.; Zhang, H.; Chen, K.; Liu, B.; Yu, Q. L.; Zhang, C. J.; Sun, J.; Yang, Q.; Zhang, X. H.; Tang, B. Z. Aliphatic Polyesters with White-Light Clusteroluminescence. *J. Am. Chem. Soc.* **2022**, *144*, 15286–15294.
- (8) Guo, L.; Yan, L.; He, Y.; Feng, W.; Zhao, Y.; Tang, B. Z.; Yan, H. Hyperbranched Polyborate: A Non-conjugated Fluorescent Polymer with Unanticipated High Quantum Yield and Multicolor Emission. *Angew. Chem., Int. Ed.* **2022**, *61*, No. e202204383.
- (9) Zhang, J.; Alam, P.; Zhang, S.; Shen, H.; Hu, L.; Sung, H. H. Y.; Williams, I. D.; Sun, J.; Lam, J. W. Y.; Zhang, H.; Tang, B. Z. Secondary Through-Space Interactions Facilitated Single-Molecule White-Light Emission from Clusteroluminogens. *Nat. Commun.* **2022**, *13*, No. 3492.
- (10) Song, C. L.; Li, Z.; Wu, J. R.; Lu, T.; Yang, Y. W. Intramolecular Through-Space Interactions Induced Emission of Pillar[4]Arene[1]-Dicyanobenzene. *Chem. Mater.* **2022**, *34*, 10181–10189.
- (11) Oprea, S.; Potolinca, V. O. Synthesis and Properties of Water-dispersible Polyurethanes Based on Various Diisocyanates and PEG as the Hard Segment. *J. Appl. Polym. Sci.* **2023**, *140*, No. e53948.
- (12) Wongsamut, C.; Suwanpreedee, R.; Manuspiya, H. Thermoplastic Polyurethane-Based Polycarbonate Diol Hot Melt Adhesives: The Effect of Hard-Soft Segment Ratio on Adhesion Properties. *Int. J. Adhes. Adhes.* **2020**, *102*, No. 102677.
- (13) Li, R.; Loontjens, J. A. T.; Shan, Z. The Varying Mass Ratios of Soft and Hard Segments in Waterborne Polyurethane Films: Performances of Thermal Conductivity and Adhesive Properties. *Eur. Polym. J.* **2019**, *112*, 423–432.
- (14) Zhong, Q.; Chen, X.; Yang, Y.; Cui, C.; Ma, L.; Li, Z.; Zhang, Q.; Chen, X.; Cheng, Y.; Zhang, Y. Hydrogen Bond Reinforced, Transparent Polycaprolactone-Based Degradable Polyurethane. *Mater. Chem. Front.* **2021**, *5*, 5371–5381.
- (15) Ma, J.; Liu, C.; Dong, Y.; Fan, Q.; Bao, Y.; Yan, H. Waterborne Polyurethane/Silica Nanocomposites Based on Electrostatic Interaction: Interfacial Interactions and Properties. *Prog. Org. Coat.* **2022**, *171*, No. 107052.
- (16) Jiang, N.; Zhu, D.; Su, Z.; Bryce, M. R. Blue-Emitting Thermoreversible polyurethane Gelators with Aggregation-Induced Emission Properties. *J. Mater. Chem. C* **2020**, *8*, 5137–5142.
- (17) Li, X.; Li, J.; Wei, W.; Yang, F.; Wu, M.; Wu, Q.; Xie, T.; Chen, Y. Enhanced Mechanochemiluminescence from End-Functionalized Polyurethanes with Multiple Hydrogen Bonds. *Macromolecules* **2021**, *54*, 1557–1563.
- (18) Jiang, N.; Ruan, S. H.; Liu, X. M.; Zhu, D.; Li, B.; Bryce, M. R. Supramolecular Polyurethane Gel with Multicolor Luminescence Controlled by Mechanically Sensitive Hydrogen-Bonding. *Chem. Mater.* **2020**, *32*, 5776–5784.
- (19) Yang, S.; Liu, J.; Cao, Z.; Li, M.; Luo, Q.; Qu, D. Fluorescent Photochromic Donor-Acceptor Stenhouse Adduct Controlled by Visible Light. *Dyes Pigm.* **2018**, *148*, 341–347.
- (20) Liu, Y.; Yang, H.; Wang, Y.; Ma, C.; Luo, S.; Wu, Z.; Zhang, Z.; Li, W.; Liu, S. Fluorescent Thermochromic Wood-Based Composite Phase Change Materials Based on Aggregation-Induced Emission Carbon Dots for Visual Solar-Thermal Energy Conversion and Storage. *Chem. Eng. J.* **2021**, *424*, No. 130426.
- (21) Ma, Y.; Yu, Y.; She, P.; Lu, J.; Liu, S.; Huang, W.; Zhao, Q. On-Demand Regulation of Photochromic Behavior through Various Counterions for High-Level Security Printing. *Sci. Adv.* **2020**, *6*, No. eaaz2386.
- (22) Li, Q.; Qiu, J.; Liu, H.; Chen, X. A Luminescent Lyotropic Liquid Crystal with UV Irradiation Induced Photochromism. *Soft Matter* **2020**, *16*, 1170–1178.
- (23) Du, J.; Sheng, L.; Xu, Y.; Chen, Q.; Gu, C.; Li, M.; Zhang, S. X. Printable Off-On Thermoswitchable Fluorescent Materials for Programmable Thermally Controlled Full-Color Displays and Multiple Encryption. *Adv. Mater.* **2021**, *33*, No. 2008055.
- (24) Yimyai, T.; Crespy, D.; Pena-Francesch, A. Self-Healing Photochromic Elastomer Composites for Wearable UV-Sensors. *Adv. Funct. Mater.* **2023**, *33*, No. 2213717.
- (25) Chen, Y.; Chen, X.; Zhao, C.; Sun, J.; Xiong, W.; Yan, K.; Zhang, Y.; He, L.; Pan, A. Highly Stable, Sensitive, and Wide-Range Temperature Sensing of Luminous Nanofibers Fabricated by in-Situ Crystallization of CsPbBr₃ within Silica for a Non-Contact Optical Temperature Probe. *Chem. Eng. J.* **2023**, *460*, No. 141772.
- (26) Wen, G. Y.; Zhou, X. L.; Tian, X. Y.; Hu, T. Y.; Xie, R.; Ju, X. J.; Liu, Z.; Pan, D. W.; Wang, W.; Chu, L. Y. Real-Time Quantitative Detection of Ultraviolet Radiation Dose Based on Photochromic Hydrogel and Photo-Resistance. *Chem. Mater.* **2022**, *34*, 7947–7958.
- (27) Peterson, C.; Hillmyer, M. A. Fast Photochromic Dye Response in Rigid Block Polymer Thermosets. *ACS Appl. Polym. Mater.* **2019**, *1*, 2778–2786.
- (28) Zhang, W.; Schenning, A. P. H. J.; Kragt, A. J. J.; Zhou, G.; De Haan, L. T. Reversible Thermochromic Photonic Coatings with a Protective Topcoat. *ACS Appl. Mater. Interfaces* **2021**, *13*, 3153–3160.
- (29) Talebi, R. Investigating Multicolor Photochromic Behaviour of AgCl and AgI Thin Films Loaded with Silver Nanoparticles. *Phys. Chem. Chem. Phys.* **2018**, *20*, 5734–5743.
- (30) Oggioni, L.; Pariani, G.; Zamkotsian, F.; Bertarelli, C.; Bianco, A. Holography with Photochromic Diarylethenes. *Materials* **2019**, *12*, 2810–2823.
- (31) Kobayashi, Y.; Abe, J. Real-Time Dynamic Hologram of a 3D Object with Fast Photochromic Molecules. *Adv. Opt. Mater.* **2016**, *4*, 1354–1357.
- (32) Cao, L.; Wang, Z.; Zong, S.; Zhang, S.; Zhang, F.; Jin, G. Volume Holographic Polymer of Photochromic Diarylethene for Updatable Three-Dimensional Display. *J. Polym. Sci., Part B: Polym. Phys.* **2016**, *54*, 2050–2058.
- (33) Zhang, R.; Jin, Y.; Yuan, L.; Deng, K.; Wang, C.; Xiong, G.; Chen, L.; Hu, Y. Inorganic Photochromism Material SrHfO₃:Er³⁺ Integrating Multiple Optical Behaviors for Multimodal Anti-Counterfeiting. *J. Alloys Compd.* **2022**, *921*, No. 166081.
- (34) Zou, D.; Li, Z.; Long, D.; Dong, X.; Qu, H.; Yang, L.; Cao, X. Molecular Cage with Dual Outputs of Photochromism and Luminescence Both in Solution and the Solid State. *ACS Appl. Mater. Interfaces* **2023**, *15*, 13545–13553.
- (35) Wu, B.; Xu, X.; Tang, Y.; Han, X.; Wang, G. Multifunctional Optical Polymeric Films with Photochromic, Fluorescent, and Ultra-Long Room Temperature Phosphorescent Properties. *Adv. Opt. Mater.* **2021**, *9*, No. 2101266.
- (36) Tian, S.; Fan, H.; Chen, Y.; Yan, J.; Sun, J.; Qin, D. A Photochromic Long Persistent Luminescent Polyurethane Based on a Color Conversion Process. *New J. Chem.* **2017**, *41*, 15405–15410.
- (37) Kang, J.; Liu, J.; Shi, F.; Dong, Y.; Jiang, S. The Thermochromic Characteristics of Zn-Doped VO₂ That Were Prepared by the Hydrothermal and Post-Annealing Process and Their Polyurethane Composite Films. *Ceram. Int.* **2021**, *47*, 15631–15638.
- (38) Wang, Z.; Hou, X.; Duan, N.; Ren, Y.; Yan, F. Shape- and Color-Switchable Polyurethane Thermochromic Actuators Based on Metal-Containing Ionic Liquids. *ACS Appl. Mater. Interfaces* **2021**, *13*, 28878–28888.
- (39) Lv, C.; Hu, L.; Yang, Y.; Li, H.; Huang, C.; Liu, X. Waterborne UV-Curable Polyurethane Acrylate/Silica Nanocomposites for Thermochromic Coatings. *RSC Adv.* **2015**, *5*, 25730–25737.
- (40) Jin, Y.; Shi, M.; Zhu, Y.; Pang, Z.; Li, X.; Ge, M. Luminescent Polyurethane Composite with Real-Time Thermal Response via Visible Signal. *Mater. Res. Express* **2021**, *8*, No. 025701.
- (41) Zhan, S.; Yang, J.; Bo, Y.; Ding, W.; Sun, Z.; Liu, H.; Wang, S.; Zhang, M. Photochromic Safety-Glass Based on Polyurethane

Interlayer Film Blend with Perovskite Quantum Dot. *Mater. Today Commun.* **2023**, *35*, No. 106015.

(42) Li, G.; Pan, Z.; Jia, Z.; Wang, J.; Zhang, N.; Pan, M.; Yuan, J. An Effective Approach for Fabricating High-Strength Polyurethane Hydrogels with Reversible Photochromic Performance as a Photoswitch. *New J. Chem.* **2021**, *45*, 6386–6396.

(43) Tian, S.; Wen, J.; Fan, H.; Chen, Y.; Yan, J. A Thermochromic Luminous Polyurethane Based on Long Persistent Luminescent Phosphors and Thermochromic Pigment. *New J. Chem.* **2018**, *42*, 5066–5070.

(44) Ji, X.; Liu, J.; Zhang, W.; Liu, W.; Wang, C. Polyurethane with Tailored Molecular Weight. *Prog. Org. Coat.* **2020**, *145*, No. 105164.

(45) Ji, X.; Zhang, W.; Ge, F.; Wang, C.; Yin, Y.; Chen, K. Thermochromic Behavior Analysis of Terminated Polyurethane Functionalized with Rhodamine B Derivative. *Prog. Org. Coat.* **2019**, *131*, 111–118.

(46) Xie, H.; Li, Z.; Gong, J.; Hu, L.; Alam, P.; Ji, X.; Hu, Y.; Chau, J. H. C.; Lam, J. W. Y.; Kwok, R. T. K.; Tang, B. Z. Phototriggered Aggregation-Induced Emission and Direct Generation of 4D Soft Patterns. *Adv. Mater.* **2021**, *33*, No. 2105113.

(47) Wang, Y. L.; Chen, K.; Li, H. R.; Chu, B.; Yan, Z.; Zhang, H. K.; Liu, B.; Hu, S.; Yang, Y. Hydrogen Bonding-Induced Oxygen Clusters and Long-Lived Room Temperature Phosphorescence from Amorphous Polyols. *Chin. Chem. Lett.* **2023**, *34*, No. 107684.

(48) Liu, X. W.; Zhao, W.; Wu, Y.; Meng, Z.; He, Z.; Qi, X.; Ren, Y.; Yu, Z. Q.; Tang, B. Z. Photo-Thermo-Induced Room-Temperature Phosphorescence through Solid-State Molecular Motion. *Nat. Commun.* **2022**, *13*, No. 3887.